Nucleic Acids Research, 2023, **51**, 11534–11548
https://doi.org/10.1093/nar/gkad838
Advance access publication date: 13 October 2023
Gene regulation, Chromatin and Epigenetics

Low RNA stability signifies strong expression regulatability of tumor suppressors

Xinlei Gao[1,2,3,†], Yang Yi[4,†], Jie Lv[3,†], Yanqiang Li[1,2,3], Kulandaisamy Arulsamy[1,2], Sahana Suresh Babu[3], Ivone Bruno[3], Lili Zhang[1], Qi Cao[4,*] and Kaifu Chen[1,2,3,5,*]

[1]Basic and Translational Research Division, Department of Cardiology, Boston Children's Hospital, Boston, MA 02115, USA
[2]Department of Pediatrics, Harvard Medical School, Boston, MA 02115, USA
[3]Houston Methodist Research Institute, The Methodist Hospital System, Houston, TX 77030, USA
[4]Department of Urology, Robert H. Lurie Comprehensive Cancer Center, Feinberg School of Medicine, Northwestern University, Chicago, IL 60611, USA
[5]Prostate Cancer Program, Dana-Farber Harvard cancer Center, Boston, MA 02115, USA

[*]To whom correspondence should be addressed. Tel: +1 617 919 5385; Email: Kaifu.Chen@childrens.harvard.edu
Correspondence may also be addressed to Qi Cao. Email: Qi.Cao@northwestern.edu
[†]The authors wish it to be known that, in their opinion, the first three authors should be regarded as Joint First Authors.

Abstract

RNA expression of a gene is determined by not only transcriptional regulation, but also post-transcriptional regulation of RNA decay. The precise regulation of RNA stability in the cell plays an important role in normal development. Dysregulation of RNA stability can lead to diseases such as cancer. Here we found tumor suppressor RNAs tended to decay fast in normal cell types when compared with other RNAs. Consistent with a negative effect of m^6A modification on RNA stability, we observed preferential deposition of m^6A on tumor suppressor RNAs. Moreover, abundant m^6A and fast decay of tumor suppressor RNAs both tended to be further enhanced in prostate cancer cells relative to normal prostate epithelial cells. Further, knockdown of m^6A methyltransferase METTL3 and reader YTHDF2 in prostate cancer cells both posed stronger effect on tumor suppressor RNAs than on other RNAs. These results indicated a strong post transcriptional expression regulatability mediated by abundant m^6A modification on tumor suppressor RNAs.

Graphical abstract

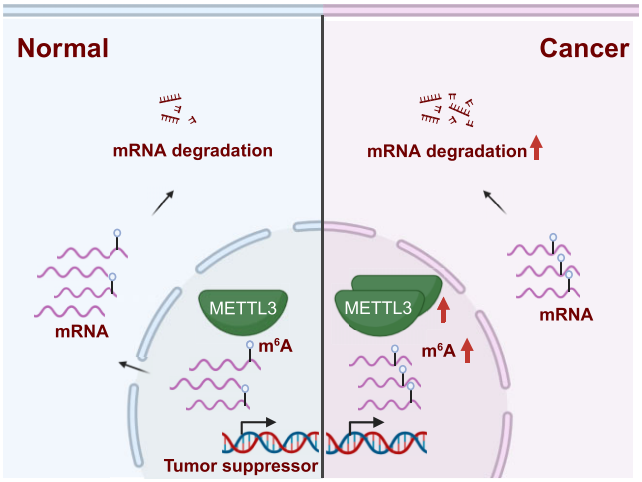

Introduction

How the genetic sequence and expression state of cancer driver genes is altered in cancer is a fundamental question. It is well known that oncogenes tend to display recurrent gain-of-function mutations in cancer, while tumor suppressors are more likely to show recessive loss-of-function mutations (1,2). However, genes that are not mutated, but with expression levels altered to cause cancers, have been frequently reported, such as the *CDKN2A* and *MLH1* (3). Therefore, the function of a cancer-related gene is determined by both DNA sequence and expression regulation in the cells.

Received: April 25, 2023. **Revised:** September 12, 2023. **Editorial Decision:** September 15, 2023. **Accepted:** September 20, 2023

The expression of a gene can be regulated at the transcriptional level by epigenetic mechanisms, e.g. DNA methylation and histone modifications (4). Cancer-related genes were recently found to display unique epigenetic modification signatures. For instance, a broad pattern of H3K4me3 was identified as enriched at tumor suppressor genes but not at oncogenes or housekeeping genes in normal cell types (5). In contrast to sharp H3K4me3 that is associated with transcription initiation, the broad H3K4me3 was linked to enhanced transcription elongation. Shortening of the broad H3K4me3 in cancer cells was found to correlate with downregulation of tumor suppressors. Moreover, broad genic repression domain (BGRD) and gene-body hypermethylation canyons in normal cell types were found to be enriched at oncogenes but not at tumor suppressor genes in normal cell types (6,7). These studies showed that tumor suppressor genes and oncogenes have distinguishable mutational and epigenetic modification patterns when compared to the rest genes in the genome.

However, the RNA expression level of a gene is determined not only by the transcription rate, but also by the post-transcriptional regulation of RNA decay (8). Changes in RNA stability can alter RNA decay rate and thus RNA abundance when transcription rate remains the same (9). Tight regulation of RNA stability is required for normal development, and dysregulation of RNA stability leads to diseases (10). Aberrant RNA stability is widespread in various types of cancer (11). Recent evidence indicated that RNA stability dysregulation of several growth factors and cell cycle regulators correlated with cancer development (12). RNA stability in the cell is regulated by epitranscriptomic factors. For instance, m^{6}A is a prevalent RNA methylation detected in mammalian mRNAs (13–15), and is reported to mediate RNA decay (16). It is yet unknown whether cancer-related genes have a unique pattern of RNA stability and thus differ from other genes in post-transcriptional regulation of their RNA expression.

In this study, we observed that tumor suppressor genes in normal cell types tend to show both frequent transcription and fast RNA decay. This feature is not observed for other analyzed gene groups such as housekeeping genes or oncogenes. We found that preferential deposition of m^{6}A modification on tumor suppressor RNAs mediated the fast RNA decay. When comparing prostate cancer cell line C4-2 to normal prostate epithelial cells (PrEC), we observed that m^{6}A-mediated fast decay of tumor suppressor RNAs were further enhanced in C4-2 cells. We further revealed that the effects of m^{6}A methyltransferase METTL3 and reader protein YTHDF2 on RNA stability are significantly stronger for tumor suppressors when compared to the rest genes. The results from these investigations demonstrated a strong RNA expression regulatability of tumor suppressor genes due to the m^{6}A-mediated low RNA stability.

Materials and methods

Cell culture

Human Prostate Epithelial Cells (PrEC) were purchased from Lonza and cultured using PrEGM Prostate Epithelial Cell Growth Medium BulletKit (Lonza). Human PCa cell line of C4-2 was a generous gift from Dr Leland Chung and grown in RPMI 1640 medium supplemented with 10% FBS. All cells were maintained at 37°C and 5% CO_2 in a humidified atmosphere and were authenticated and routinely screened for Mycoplasma.

Lentivirus construction

The lentiviral shRNA vectors used here were purchased from Sigma (shMETTL3: TRCN0000289742; shYTHDF2: TRCN0000265510). For lentivirus production, shRNA vectors and helper plasmids of pVSVG and psPAX2 were co-transfected into HEK293T cells using Lipofectamine 3000 (Invitrogen) following its protocol. The medium was renewed once at 24 h post-transfection. The supernatants containing viruses were collected at 48 h post-transfection and directly used for infection.

Time-series RNA-Seq upon actinomycin D (ActD) treatment

PrEC and C4-2 cells were treated with transcription inhibitor actinomycin D (ActD, Sigma) at a concentration of 5 μg/ml for 0, 15 min, 1 h and 2 h. RNA samples were then isolated using RNeasy Plus Mini Kit (Qiagen) and sent to BGI for library preparation and follow-up sequencing. Human primary total T cells were isolated from the blood sample of three donors from Gulf Coast Regional Blood Center using Ficoll density gradient method. The cells were collected and washed with PBS + 0.5% FBS and taken into culture. After isolation, the cells were activated with anti-CD3/CD28 microbeads (Thermo Fisher) for 24 h. For transcription inhibition, the cultured cells were treated with ActD (10 μg/ml), for four time points, 0 h (immediately after ActD treatment), 15 min, 1 h and 2 h. After treatment, RNA was isolated by RNeasy kit (Qiagen). The total RNA-seq library construction was performed by RNA core.

Methylated (m^{6}A) RNA immunoprecipitation sequencing (MeRIP-seq)

To monitor the status of m^{6}A and map the location of m^{6}A RNA modifications transcriptome-wide, the MeRIP-seq was conducted in duplicates using Magna MeRIP™ m^{6}A Kit (Millipore) with the procedure provided by the manufacturer. In brief, the total RNA from C4-2 and PrEC cells was extracted using RNeasy Plus Mini Kit (Qiagen), followed by mRNA isolation using PolyATtract mRNA Isolation System (Promega). The obtained mRNA was fragmented into ∼100 nt in length and purified by miRNeasy Mini Kit (Qiagen). After incubation with anti-m^{6}A antibody-magnetic beads mixture at 4°C overnight, the m^{6}A-modified mRNA fragments bound to beads were eluted and shipped to BGI for library preparation and sequencing using the DNBseq platform.

Western blot

Proteins in cell lysates were denatured by adding 4 × loading buffer (Bio-Rad) followed by incubation at 95°C for 10 min. Then, the protein samples were separated electrophoretically by SDS-PAGE, and semi-dry transferred to nitrocellulose membranes (Bio-Rad). After blocking for 30 min in Tris-buffered saline-Tween 20 (TBST) with 5% nonfat milk, the membranes were subjected to immunoblotting by incubation with primary antibodies for 2 h at room temperature. Then, the membranes were washed and incubated with goat anti-mouse/rabbit IgG (H + L)-HRP secondary antibody (GenDEPOT, 1:5000 dilution) for 1 h. The signals were

developed using western ECL Substrate (Bio-Rad) and captured by a Bio-Rad imaging system. The primary antibodies used in this paper were listed in Supplementary Table S1.

Isolation and detection of nascent RNA

The newly minted RNAs were enriched using Click-iT Nascent RNA Capture Kit (Thermo) by following manufacturer's manual. In general, the nascent RNAs were firstly labeled by incubation of live cells with 5-ethynyl uridine (EU) for 6 h. After incubation, the total RNA containing EU-labeled nascent RNA was isolated using RNeasy Plus Mini Kit (Qiagen) and used in a copper catalyzed click reaction with an azide-modified biotin. The captured nascent RNA transcripts on streptavidin magnetic beads were reverse transcribed using the SuperScript VILO cDNA synthesis kit (Thermo). The resulting cDNAs were then subjected to Real-time (RT)-qPCR analyses using Universal SYBR Green Supermix (Bio-Rad) in the QuantStudio 6 Flex Real-time PCR System (GE Healthcare) following manufacturer's instructions. All primers used for RT-qPCR analysis were summarized in Supplementary Table S2. The relative RNA level was calculated using the $2^{-\Delta\Delta Ct}$ method with the Ct values normalized using GAPDH as an internal control.

Quantification of global m^{6}A methylation level in RNA

The m^{6}A methylation levels in PrEC and C4-2 cells were measured using EpiQuik m^{6}A RNA Methylation Quantification Kit (EPIGENTEK) according to the manufacturer's instructions. In brief, 200 ng of total RNA were used for each sample and the m^{6}A contents were quantified by reading the absorbance of each sample at 450 nm.

Transfection of siRNA

All the silencer siRNAs used in this study were purchased from Thermo Fisher (siMETTL3-1: s32141, siMETTL3-2: s32142; siYTHDF2-1: s28147, siYTHDF2-2: s28148). Lipofectamine RNAiMAX (Invitrogen) was utilized for siRNA transfection according to the manufacturer's protocol. Cells were collected at 3 days post-transfection for further use.

Measurement of viability and apoptosis upon METTL3 or YTHDF2 suppression

The ApoTox-Glo Triplex Assay (Promega) was utilized to access the viability and apoptosis simultaneously by following the manufacturer's instructions. In brief, control, siMETTL3 and siYTHDF2 C4-2 cells were seeded into 96-well plate for a final volume of 100 μl per well. The ApoTox-Glo Triplex Assay was then performed at each time-point, in which the fluorescence (Viability) and luminescence (Apoptosis) were measured using a Tecan plate reader.

RNA-seq data analysis

RNA-Seq reads were mapped to human reference genome version hg19 using TopHat (version v2.0.12) (17) with default parameters. Next, Cuffdiff (version 2.2.1) (18) was used to generate read count matrix. Normalized gene expression values in FPKM (fragments per kilobases per million mapped reads) was further calculated using UCSC knownGene as the reference genes. Genes with FPKM value larger than one were retained for further analysis. Differential expression test was performed using edgeR (19). Heatmaps showing gene expression changes were generated by the R package pheatmap (version 1.0.12). RNA-seq genome browser tracks were visualized by IGV (20).

Calculation of RNA stability

RNA stability was calculated based on pairwise differential expression analysis between the time points 0 and each other time point during ActD treatment. The stability value was determined by summing the absolute values of log transformed Q-value of each pairwise differential expression test between control sample and each sample treated with ActD (21). Genes were ranked by their mRNA stability scores from low to high and divided into gene sets of equal size. The enrichment of tumor suppressors, oncogenes and housekeeping genes in a certain gene set was measured by Fisher exact test.

mRNA half-life of genes was calculated using the method described previously (22). Briefly, gene expression values (FPKM) were used to calculate log2 fold change between the time points 2-h and 0-h. It was observed that genes with the most stable RNAs can have increased expression levels even after transcription inhibition. To remove this noise and eliminate the expression increase in the most stable mRNAs, we further normalized gene expression data by summing the expression values of the top 10 most stable mRNAs. Subsequently, mRNA half-life was calculated using the formula as listed in (23). In short, the RNA decay rate K_{decay} was estimated by the ratio of FPKM value changes over each time periods. The half-life was then calculated as $\ln 2/K_{decay}$. The average half-life over 0 h, 15 min, 1 h and 2 h was defined as the final half-life.

Functional enrichment analysis

KEGG pathway enrichment analysis for the most stable and unstable genes were performed by DAVID online analysis (24). The gene list was filtered by GREAT (Genomic Regions Enrichment of Annotations Tool) version 2.0 to retain the well annotated genes for further analysis. The pathways with Benjamini adjusted P value smaller than 0.001 and gene number larger than 10 was defined as significantly enriched.

Analysis of ChIP-Seq data

PrEC ChIP-Seq data for RNA polymerase II (Pol II), H3K4me3, H3K9K14ac, H3K36me3 and H3K27ac, were downloaded from NCBI GEO database (accession numbers listed in Supplementary Table S3). Reads were filtered by Trimmomatic (25) to remove low-quality bases with parameters ILLUMINACLIP:TruSeq3-SE:2:30:10 LEADING:3 TRAILING:3 SLIDINGWINDOW:4:15 MINLEN:36. Then the clean reads were mapped to human genome (version hg19) by Bowtie (26), and only reads mapped to a unique position in the genome were retained for further analysis. Number of reads mapped to the 2 kb nearby region around transcription start sites (TSSs) or the whole gene body was counted by SAMtools using the UCSC knownGene for the human genome version hg19 as the reference genes. Peak calling was performed using MACS2 (27). Wig files were generated by DANPOS2 (version 2.2.2) (28) as described in previous studies (6,29). To calculate correlation between RNA stability and density of histone marks, all genes were ranked by RNA stability from low to high and then divided into 500 bins, with around 20 genes in each bin to calculate an average value. After binning,

spearman correlation coefficient was calculated between histone mark density and RNA stability.

MeRIP-Seq analysis and m^{6}A profile in gene bodies

MeRIP-Seq libraries were generated using PrEC cells, C4-2 control (shCTRL) cells and C4-2 METTL3-knockdown (shMETTL3) cells. MeRIP-Seq data (two replicates) was filtered by Trimmomatic (25) to remove low-quality bases and then mapped to human genome (version hg19) by Tophat (version v2.0.12) using default parameters. The read coverage calculation and normalization were conducted by deepTools (30). The distribution of m^{6}A signal across gene body (5′ UTR, CDS and 3′ UTR) was measured by FPKM values in bins by deepTools. The normalized IP signal per bin was subtracted by normalized input signal to generate m^{6}A signal coverage plot (30). To filter out potential noise in gene annotation and obtain more precise profiles of m^{6}A across gene body, we utilized NCBI Refseq gene annotation and considered that some genes may have multiple transcripts with different start site of 3′ UTR, only the transcript with the leftmost start site of 3′ UTR was retained for each gene. Then overlapping transcripts and transcripts with 5′ UTR or 3′ UTR shorter than 50 bp were removed. The retained transcript annotation was next utilized to create slide windows to investigate the profile of m^{6}A signal distributions (15). Enrichment peaks of m^{6}A signal were called by MACS2 (27) and exomePeak2 using default parameters. m^{6}A peaks called by MACS2 required q-value <0.05, and by exomePeak2 q-value <0.1. Differential methylation sites were identified by exomePeak2.

PRO-Seq data analysis

The PRO-Seq dataset of MCF-7 cell line was download from NCBI GEO database with the accession number GSE144404 (https://www.ncbi.nlm.nih.gov/geo/query/acc.cgi?acc=GSE144404) (31). The data was analyzed following the method reported by Xu *et al.* (31). Briefly, adaptors and low-quality reads were removed from raw data using fastp (32). The reads mapping to ribosomal RNAs by bowtie2 (26) were further removed from the clean reads. Next, the remaining reads were mapped to the *Drosophila* genome (version dm6) and human genome (version hg19) using bowtie2. Strand specific alignments with the flags of 99, 147, 83 and 163 were retrieved by samtools (version 1.16.1) (33). Reads mapping to the *Drosophila* genome and human genome were counted with htseq-count (version 0.11.2) (34). The read counts aligned to the *Drosophila* genome were used for spike-in normalization. The normalization factors were calculated as the minimum spike-in read count across all the samples divided by the spike-in read count of each sample. The normalized read counts of the human genome were then used to perform differential expression analysis by Poisson test.

Results

Tumor suppressor RNAs tend to decay fast in normal non-cancer cells

To measure RNA stability across the transcriptome, here we sequenced oligo dT-selected RNA (PolyA RNA-seq) from a series of normal prostate epithelial cells (PrEC) samples. These include samples in which the transcription was inhibited by treating the cells with actinomycin D (ActD) for 15, 60 and 120 min. A sample with no (0 minute) inhibition of transcription was sequenced as the control (Figure 1A). To define RNA stability based on decay rate (see Materials and Methods), we analyzed the 12180 genes that showed more than one fragment Per Kilobase of exon per Million mapped fragments (FPKM) in the control sample. The analysis revealed a wide variation of RNA decay rate. Whereas the expression levels of the most stable RNAs showed no decrease after 120 min, the abundance of many RNAs had decreased at as early as 15 min (Figure 1B). Interestingly, by manual inspection of the RNA-Seq data, we observed that tumor-suppressor RNAs tended to decay fast. For instance, the tumor suppressors *CDKN1B* (35) and *IRF2BP2* (36) showed progressive reduction of RNA level by 7- and 8-fold after inhibition of transcription for 120 min, respectively (Figure 1C). In contrast, RNAs of housekeeping genes are more likely to be stable, e.g. the RNA levels of *PEX6* (37) and *ACTB* (38) were still not reduced after the inhibition of transcription for 120 min (Figure 1C). This result highlighted the heterogeneity of RNA decay rates among genes, prompting us to explore the functional implication of the RNA decay landscape in PrEC.

We next systematically investigated the functional relevance of RNA decay rate. We retrieved the top 1000 genes of the most unstable RNAs for a comparison to the 1000 genes of the most stable RNAs (Figure 1B and Supplementary Table S4). We then performed a Kyoto Encyclopedia of Genes and Genomes (KEGG) pathway analysis for the two gene groups (Figure 1D). Although the analysis was performed in the normal prostate epithelial cells PrEC, we observed significant enrichment of cancer pathways in the genes of the most unstable RNAs. In contrast, housekeeping pathways were enriched in the genes of the most stable RNAs, e.g. the Metabolic pathways (hsa01100) and Oxidative phosphorylation pathway (has00190). The cancer-related functions of genes in the cancer pathways were manually curated by the developers of the KEGG database based on literature report (Supplementary Table S5). To further verify the association between RNA stability and cancer-related genes, we analyzed an additional set of cancer-related genes defined in a different way. It includes 500 tumor suppressors and 500 oncogenes defined by the TUSON algorithm based on DNA mutation patterns ($P = 1.03 \times 10^{-2}$) in 8200 tumor-normal sample pairs (39) (Supplementary Table S5). For comparison, we also analyzed 500 randomly selected genes and a set of housekeeping genes defined in a recent literature (37) (Supplementary Table S5). We observed that the tumor suppressor genes showed a strong enrichment in the genes of the most unstable RNAs (Figure 1E). Specifically, the enrichment of the 1000 genes of the most unstable RNAs were 4.4-fold (one-tailed Fisher's exact test Bonferroni corrected P value 5.1×10^{-28}) for the tumor suppressor genes (15.8%) when compared to the randomly selected control genes (3.6%). The enrichment weakened sharply in the genes of stabler RNAs. Specifically, the tumor suppressors were slightly enriched in the second (3.2-fold, 11.6%, $P = 3.6 \times 10^{-14}$) and third (3.0-fold, 10.8%, $P = 6.2 \times 10^{-12}$) 1000-genes groups. In contrast, no significant enrichment for oncogenes were observed in these gene groups. Housekeeping genes showed a slight enrichment in most of the 1000-genes groups defined by their different levels of RNA stability. The strongest enrichment (2.9-fold, $P = 6.7 \times 10^{-11}$) of housekeeping genes was observed in the gene group with a median level of RNA stability. These results indicated that the RNAs of tumor suppressors tend to be unstable when compared to other genes expressed in PrEC. Notably, tumor

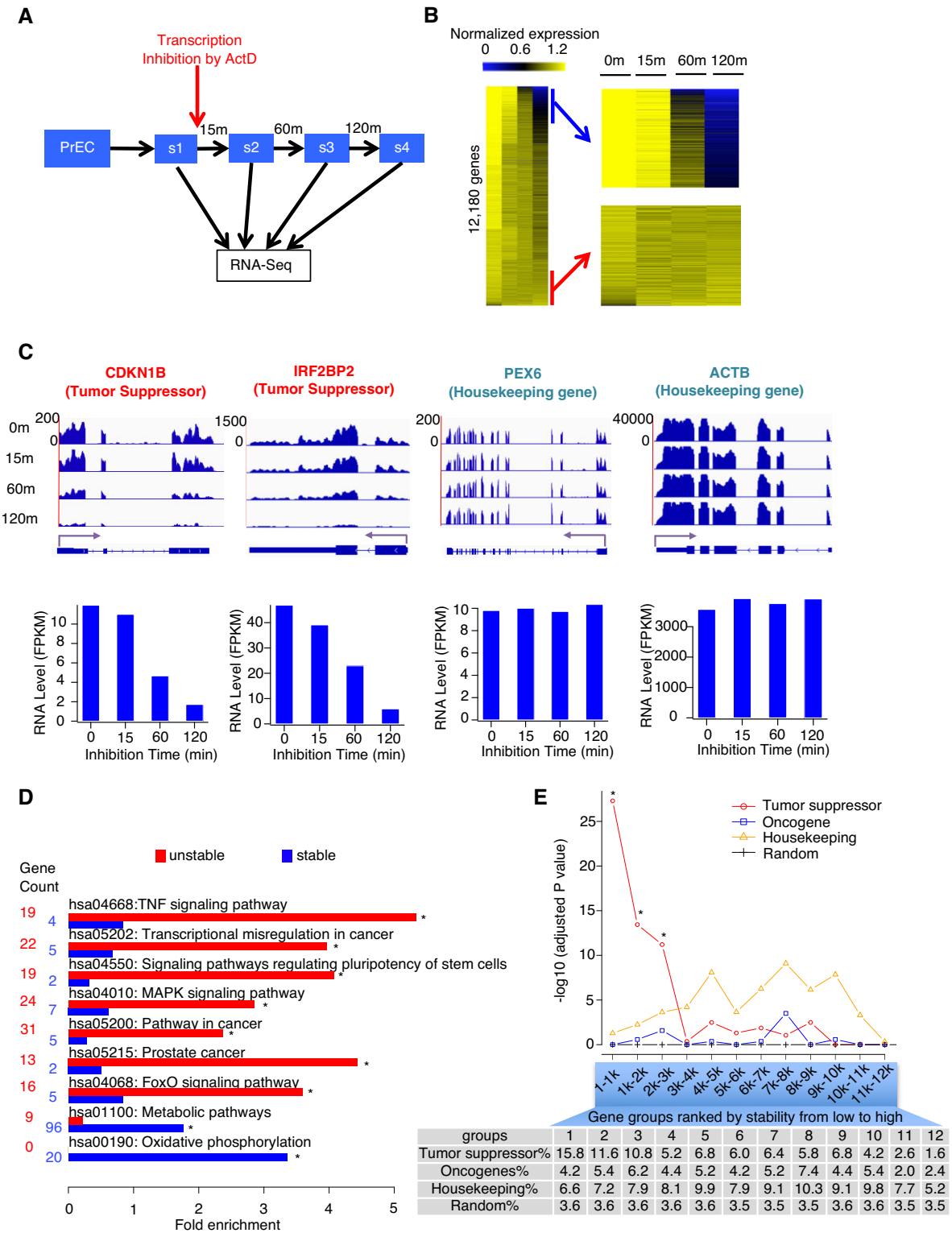

groups	1	2	3	4	5	6	7	8	9	10	11	12
Tumor suppressor%	15.8	11.6	10.8	5.2	6.8	6.0	6.4	5.8	6.8	4.2	2.6	1.6
Oncogenes%	4.2	5.4	6.2	4.4	5.2	4.2	5.2	7.4	4.4	5.4	2.0	2.4
Housekeeping%	6.6	7.2	7.9	8.1	9.9	7.9	9.1	10.3	9.1	9.8	7.7	5.2
Random%	3.6	3.6	3.6	3.6	3.6	3.5	3.5	3.5	3.6	3.6	3.5	3.5

Figure 1. Tumor suppressor genes tend to have a low RNA stability. (**A**) The flowchart of RNA-Seq experiments to profile RNA decay rate. (**B**) Heatmap to show RNA expression value of individual genes (rows) at individual time points during transcription inhibition. (**C**) RNA-Seq reads density (top panels) and FPKM value (bottom panels) of example genes. (**D**) KEGG pathway enrichment analysis for top 1000 genes of the most unstable transcripts (red) and top 1000 genes of the most stable transcripts (blue). *, Benjamini corrected one sided Fisher's exact test *P* value <0.001. (**E**) The adjusted enrichment P value and percentage of tumor suppressors, oncogenes, housekeeping genes and randomly selected control genes in individual gene groups ranked by their RNA stability from low to high. *, Bonferroni corrected one sided Fisher's exact test *P* value $< 1 \times 10^{-10}$.

suppressor genes encompass various distinct categories, such as those in the DNA damage repair, cell cycle checkpoints, and signaling pathways. A common trend of low RNA stability was observed among tumor suppressors across these subcategories (Supplementary Figure S1 and Supplementary Table S6).

The fast RNA decay of tumor suppressors is a feature conserved across cell types

We questioned whether tumor suppressor RNAs also tend to be unstable in cell types other than PrEC. Therefore, we further performed RNA-Seq to profile RNA stability in human primary T-cells. To test if the observation was affected by different RNA-Seq protocols, we performed both PolyA RNA-seq (Supplementary Figure S2A and B) and rRNA-depleted whole-cell RNA sequencing (Total RNA-seq, Supplementary Figure S3A and B). We found the results consistent between PrEC and T cells, and consistent between the PolyA RNA-Seq and Total RNA-Seq. Manual inspection revealed that the unstable and stable RNAs in PrEC also tended to be unstable and stable in T cells, respectively (Supplementary Figure S2C, Supplementary Figure S3C). Significant enrichment of cancer-related pathways in the genes of the most unstable RNAs was also observed in T-cells (Supplementary Figure S2D, Supplementary Figure S3D). Enrichment in genes of unstable RNAs was observed for tumor suppressors but not for oncogenes (Supplementary Figure S2E, Supplementary Figure S3E). Therefore, tumor suppressors tended to have a low RNA stability in both PrEC and T cells.

We next aim to investigate the conservation of association between tumor suppressors and low RNA stability in several additional cell types. To this end, we analyzed 11 sets of data from 8 cell types (Supplementary Table S3). We retrieved the 1000 genes of the most unstable RNAs from each of the 11 datasets. Only tumor suppressors but not oncogenes or housekeeping genes appeared to be significantly enriched in each of these 1000-genes groups from the individual datasets (Figure 2A). By combining all these datasets, we confidently quantified RNA decay rate for 7912 genes that expressed in all these cell types, i.e. with a FPKM value greater than 1 in all 11 datasets before the inhibition of transcription. We ranked genes by median level of RNA decay rate across the 11 datasets from high to low. We then divided these genes into eight groups, with each group contained 989 genes. Therefore, the groups I to VIII corresponded to genes with RNA stability from the lowest to the highest (Figure 2B). When compared with randomly selected genes, tumor suppressors were significantly enriched (17.8%, 5.1-fold, one-tailed Fisher's exact test $P = 8.5 \times 10^{-37}$) in the gene group of the most unstable RNAs (Figure 2C). The enrichment decreased sharply in the gene groups with stronger RNA stability. Specifically, there is a less significant enrichment (13.0%, 3.7-fold, $P = 3.7 \times 10^{-19}$) in the group II, slight enrichment in groups III (8.6%, 2.5-fold, $P = 4.4 \times 10^{-7}$) and IV (8.4%, 2.4-fold, $P = 1.2 \times 10^{-6}$), and little enrichment in any of the other four groups. Also, little enrichment was observed for oncogenes or random control genes in any of these eight gene groups. For instance, we found *CDKN1B*, a tumor suppressor controlling cell cycle progression (35), exhibited high RNA decay rates in all these 11 datasets (Figure 2D). In contrast, the RNA of the oncogene *CDK4* (40) appeared to be highly stable in these datasets (Figure 2E). These results indicated that RNAs of tumor suppressors are characterized by low RNA stability across different cell types.

Some genes can be oncogenes in certain contexts and tumor suppressors in others. Although we lack a curated large group of such genes to perform statistical analysis of general feature, manual inspection of individual examples indicated that the RNA stability of these genes tended to vary across different cell types. For example, the *KLF4* gene acts as a putative tumor suppressor in prostate cancer (41), cervical cancer (42), and liver cancer (43), but as a potential oncogene in some other cancers. In breast cancer, *KLF4* can act as either tumor suppressor or oncogene in a context-dependent manner (44,45). We observed that the RNA stability of *KLF4* is highly variable across the normal and cancer cell lines used in this study, ranging from the top 0.3% to 31.1% most unstable among all the expressed RNAs (Supplementary Figure S4). Specifically, the RNAs of *KLF4* decayed fast after transcription inhibition in C4-2 cells (prostate cancer), Hela cells (cervical cancer), Huh cells (liver cancer) and MCF-7 cells (breast cancer) (Supplementary Figure S4A). The RNA stability of *KLF4* was ranked as the top 0.3% to 4.3% most unstable among all the expressed RNAs in these four cancer cell lines (Supplementary Figure S4B). Meanwhile, we observed no detectable RNA expression of *KLF4* in the T cells and HepG2 cells (liver cancer) (Supplementary Figure S4B).

Fast decay of tumor suppressor RNAs is associated with frequent transcription

Intuitively, we might expect a fast RNA decay to be associated a low steady state RNA expression level, i.e. the RNA abundance determined in the control cells without an inhibition of transcription. However, we observed little correlation between the decay rate and steady state expression level of RNAs, e.g. with a Spearman correlation coefficient 0.05 ($P = 0.25$) in PrEC (Supplementary Figure S5A). This observation could be reasonable, as the RNA expression level of a gene is orchestrated by both the transcription frequency and RNA decay rate (46). Therefore, two genes with the same RNA steady state expression level might display different RNA turnover patterns – one gene might have both low transcription frequency and low RNA decay rate, whereas the other gene might have both high transcription frequency and high RNA decay rate (Supplementary Figure S5B).

Some epigenetic features have been reported as correlative to gene transcription activity (47). To investigate the relationship between transcription rate and RNA decay rate, we analyzed several PrEC epigenomics datasets. These include ChIP-Seq data for the polymerase II (Pol II) and a set of histone modifications known to reflect transcriptional activity. We observed a strong negative Spearman correlation ($r = -0.58$, $P < 2.2 \times 10^{-16}$) between the binding density of Pol II at gene loci and the RNA stability of the associated genes (Supplementary Figure S5C, left panel). Pol II binding density was higher at the gene loci of unstable RNAs than those of stable RNAs (Supplementary Figure S5C, middle panel). Similarly, we observed negative correlations between RNA stability and histone modifications associated with transcriptional activation, including H3K4me3 ($r = -0.569$, $P < 2.2 \times 10^{-16}$), H3K36me3 ($r = -0.623$, $P < 2.2 \times 10^{-16}$), H3K9K14ac ($r = -0.718$, $P < 2.2 \times 10^{-16}$) and H3K27ac ($r = -0.658$, $P < 2.2 \times 10^{-16}$) (Supplementary Figure S5D–G, left panels). The density of these histone modifications was higher on genes

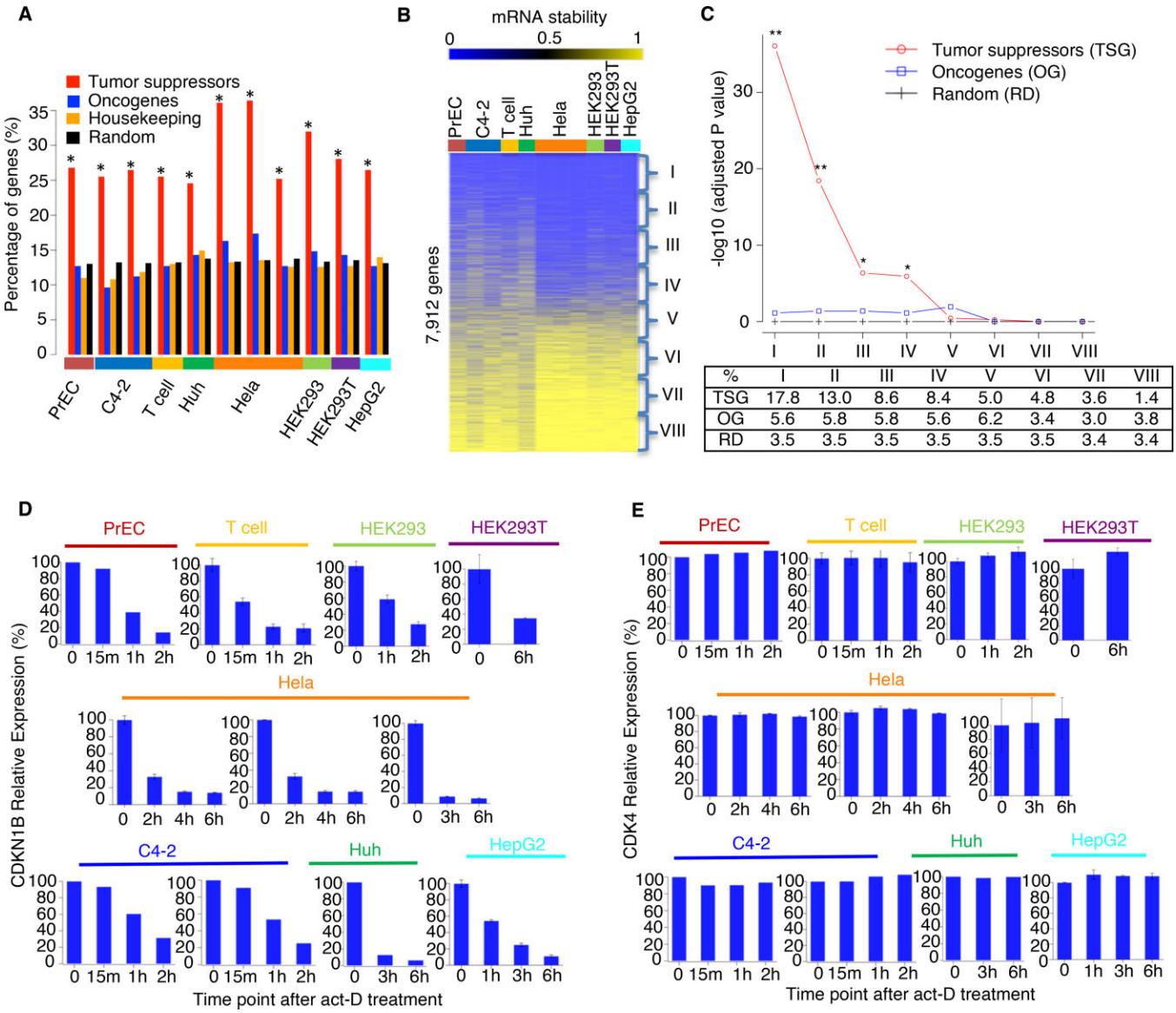

Figure 2. The low RNA stability of tumor suppressors tends to be conserved across cell types. (**A**) Bar plot to show the percentages of tumor suppressors, oncogenes, housekeeping genes and randomly selected control genes in top 1000 genes of the most unstable transcripts in each sample. $*P$ value $< 1 \times 10^{-20}$. (**B**) Heatmap to show RNA stability score of individual genes (rows) in individual samples. (**C**) The adjusted P value and percentage of tumor suppressors, oncogenes, and randomly selected control genes in each of the eight gene groups shown in (B). $**P$ value $< 1 \times 10^{-10}$. $*P$ value $< 1 \times 10^{-5}$. (D, E) The relative RNA expression levels of CDKN1B (**D**) and CDK4 (**E**) in individual datasets. Error bar indicates standard deviation. Biological replicates $n = 1$ for PrEC, C4-2 and Huh samples; $n = 2$ for HEK293, HEK293T, HeLa and HepG2 samples; $n = 3$ for T cells. P values calculated based on one tail Fisher's exact test (A, C). When applicable, P values were adjusted by the Bonferroni method (C).

of unstable RNAs than those of stable RNAs (Supplementary Figure S5D–G, middle panels). Further, the binding intensity of Pol II and density of activating histone modifications were higher at tumor suppressor genes than at oncogenes (Supplementary Figure S5C–G, right panels). This is consistent with the enrichment of tumor suppressor genes in the genes of unstable RNAs. Together, these data indicated that a low RNA stability is overall associated with strong signals of transcription activity but not a low steady state RNA expression.

It is worth noting that Pol II has different phosphorylation patterns during transcription. Pol II with Ser 5 phosphorylation (Ser-5P) is primarily at promoter regions (paused Pol II), while the Poll II with Ser 2 phosphorylation (Ser-2P) is located in coding regions and correlated with transcription elongation (elongating Pol II) (48). It is Pol II Ser-2P that is associated with active transcription elongation. Hence, we collected Pol II Ser-2P ChIP-Seq data in the MCF-7 cell line from the GEO database (accession number GSE142010). The Pol II Ser-2P profiles showed that its signal is higher in the gene body regions of unstable RNAs when compared with stable RNAs (Supplementary Figure S6A); also, it is higher in gene body regions of tumor suppressors when compared with oncogenes (Supplementary Figure S6B). These results consistently supported our conclusion that unstable RNAs and tumor suppressors tended to have higher transcription rates.

We then decided to investigate the relationship between RNA stability and RNA expression level in an improved manner. We selected two groups of genes that have similar Pol II binding density but different RNA expression level in PrEC (Supplementary Figure S7A). We observed that the group with

a higher RNA expression level displayed a stronger RNA stability (Two-tailed Wilcoxon rank sum test $P = 8.7 \times 10^{-4}$). We further selected two groups of genes with similar Pol II binding density but different RNA stability. The group with stronger RNA stability displayed higher RNA expression level (two-tailed Wilcoxon rank sum test $P = 3.4 \times 10^{-11}$) (Supplementary Figure S7B). Therefore, when transcription frequency is the same, RNA stability is a strong determinant of RNA expression level in the cell.

The fast decay is linked to preferential m^{6}A modification on tumor suppressor RNAs

RNA stability within the cell is a complex process that is subject to regulation by a multitude of factors (49). In particular, epitranscriptomic factors have emerged as key players in this regulatory network (50). Through their ability to modify RNA molecules, these factors can influence the stability of RNA and thereby impact gene expression and cellular function (51). For instance, m^{6}A is a prevalent RNA methylation detected in mammalian mRNA (13–15), and is reported to mediate RNA decay (16). However, a general connection between m^{6}A methylation and tumor suppressor RNAs was not defined before. The low RNA stability of tumor suppressors led us to hypothesize that tumor suppressor RNAs might be a set of preferential targets of m^{6}A modification. We therefore performed MeRIP-seq (14,15) to analyze m^{6}A in the prostate cancer cell line C4-2. Consistent with prior knowledge (14,15), the m^{6}A intensity appeared to be significantly higher (two-tail Wilcoxon rank sum test $P = 6.6 \times 10^{-4}$) on unstable RNAs than on stable RNAs (Figure 3A). Metagene analysis verified the enrichment of m^{6}A reads over input reads near the stop codon position of unstable RNAs but not stable RNAs (Figure 3B). Notably, RNAs of tumor suppressor genes displayed higher m^{6}A density when compared to RNAs of oncogenes (1.4-fold, one-tail Kolmogorov–Smirnov test $P = 3.7 \times 10^{-6}$) or random control genes (1.2-fold, one-tail Kolmogorov–Smirnov test $P = 0.048$) (Figure 3C). This preferential m^{6}A modification on tumor suppressor RNAs is also revealed by analyzing m^{6}A enrichment peaks. We detected m^{6}A peaks on RNAs of a significantly large percentage of tumor suppressor genes (2.3-fold enrichment, one tail Fisher's exact test $P = 8.8 \times 10^{-45}$). In contrast, we detected m^{6}A peaks on RNAs of only a slightly large percentage of oncogenes (1.2-fold enrichment, one tail Fisher's exact test $P = 0.01$) (Figure 3D). For instance, fast RNA decay and high m^{6}A modification levels were observed for the tumor suppressors *AXIN1* (52), *CDKN1B* (35) and *ARID1A* (53)(Figure 3E). Similarly, we also found this preferential m^{6}A mediated low RNA stability for tumor suppressors in another cell line, HEK293T, derived from human embryonic kidney cells (Supplementary Figure S8).

Depletion of m^{6}A regulators showed preferential effect on tumor suppressor RNAs

We next tested the role of m^{6}A in preferential destabilization of tumor suppressor RNAs in the cell. To this end, we examined whether a manipulation of m^{6}A regulators will have stronger effect on tumor suppressor RNAs than on most of the rest RNAs. METTL3 is the major enzyme that catalyzes m^{6}A on RNAs (54). To investigate the effect of *METTL3* depletion, we successfully knocked down METTL3 in C4-2 cells (Supplementary Figure S9A). We first verified that knockdown of METTL3 in C4-2 cells caused a global decrease of m^{6}A level (Figure 3F). The m^{6}A level dropped significantly in the CDS region (two-sided Wilcoxon test $P = 7.3 \times 10^{-14}$). We detected 1167 differential sites of m^{6}A across the transcriptome. Among these, 998 (85.5%) sites were defined by decrease of m^{6}A upon the knockdown of METTL3 (Figure 3G). Also, the RNAs with decreased m^{6}A tended to show decreased decay rate and thus longer RNA half-life (Figure 3H). This result confirmed the widespread effect of m^{6}A on RNA stability. Finally, we observed that depletion of *METTL3* resulted in a stronger inhibition effect on RNA decay of tumor suppressors when compared with oncogenes (one-tail Kolmogorov–Smirnov test $P = 6.1 \times 10^{-7}$) and random control genes (one-tail Kolmogorov–Smirnov test $P = 0.001$) (Figure 3I).

We further knocked down YTHDF2, a m^{6}A reader that mediates RNA decay (16). The successful knockdown of YTHDF2 in C4-2 cells was verified by western blot (Supplementary Figure S9B). We observed that knockdown of YTHDF2 caused a significant increase of RNA stability for tumor suppressors (one-tail Kolmogorov–Smirnov test $P = 2.0 \times 10^{-22}$) (Figure 3J). We next analyzed the enrichment level of tumor suppressor genes in genes with the most unstable RNAs in each of four C4-2 samples (Figure 3K). We observed a significant enrichment in the two control samples (one tailed Fisher exact test $P = 9.0 \times 10^{-22}$ for C4-2 cells, $P = 3.4 \times 10^{-25}$ for C4-2 shCTRL cells). In contrast, less enrichment was observed in the cells with METTL3 knockdown ($P = 1.1 \times 10^{-9}$). Further, no significant enrichment was observed in the cells with YTHDF2 knockdown ($P = 0.39$). We also analyzed the enrichment level of housekeeping genes or oncogenes in the genes of the most unstable RNAs in these samples. The enrichment levels of these two gene groups were not influenced by the knockdown of METTL3 and YTHDF2 in the C4-2 samples. Moreover, we assessed the impact of METTL3 or YTHDF2 knockdown on cancer cell phenotype in C4-2 cells. Depletion of METTL3 or YTHDF2 led to significantly inhibited cell growth (Supplementary Figure S9C) along with increased apoptosis (Supplementary Figure S9D). Taken together, we conclude that RNAs of tumor suppressors were assigned to a fast track of RNA decay, which can be mediated by their abundant m^{6}A modification.

Above all, our investigations of m^{6}A function were focused on the role in tumor suppressor RNA decay. It was reported that RNA modifications including m^{6}A methylation could play a role in regulation of translation (55,56). Therefore, the perturbation of m^{6}A regulators might also impact protein abundance of tumor suppressor genes. To test this hypothesis, we performed western blot to examine the protein expression changes of a set of tumor suppressor genes in response to METTL3 KD and YTHDF2 KD in C4-2 cells (Supplementary Figure S10A). To select tumor suppressors that can be potential targets of m^{6}A regulators, we chose the candidates by the three criteria: (i) contain m^{6}A peaks in at least one of the PrEC or C4-2 samples; (ii) exhibit increased RNA half-lives in response to either METTL3 KD or YTHDF2 KD and (iii) have antibodies available for western blot. By these criteria, we tested four tumor suppressor genes that contain m^{6}A modifications in their RNAs and show low RNA stability, including *KLF4*, *BAX*, *CDKN1B* and *SETD7*. Three of the four genes except *SETD7* showed a slight increase of mRNA half-life in response to METTL3 KD (Supplementary Figure S10B), whereas all four genes exhibited about 1.6–3-fold increase of mRNA half-life in response to YTHDF2 KD

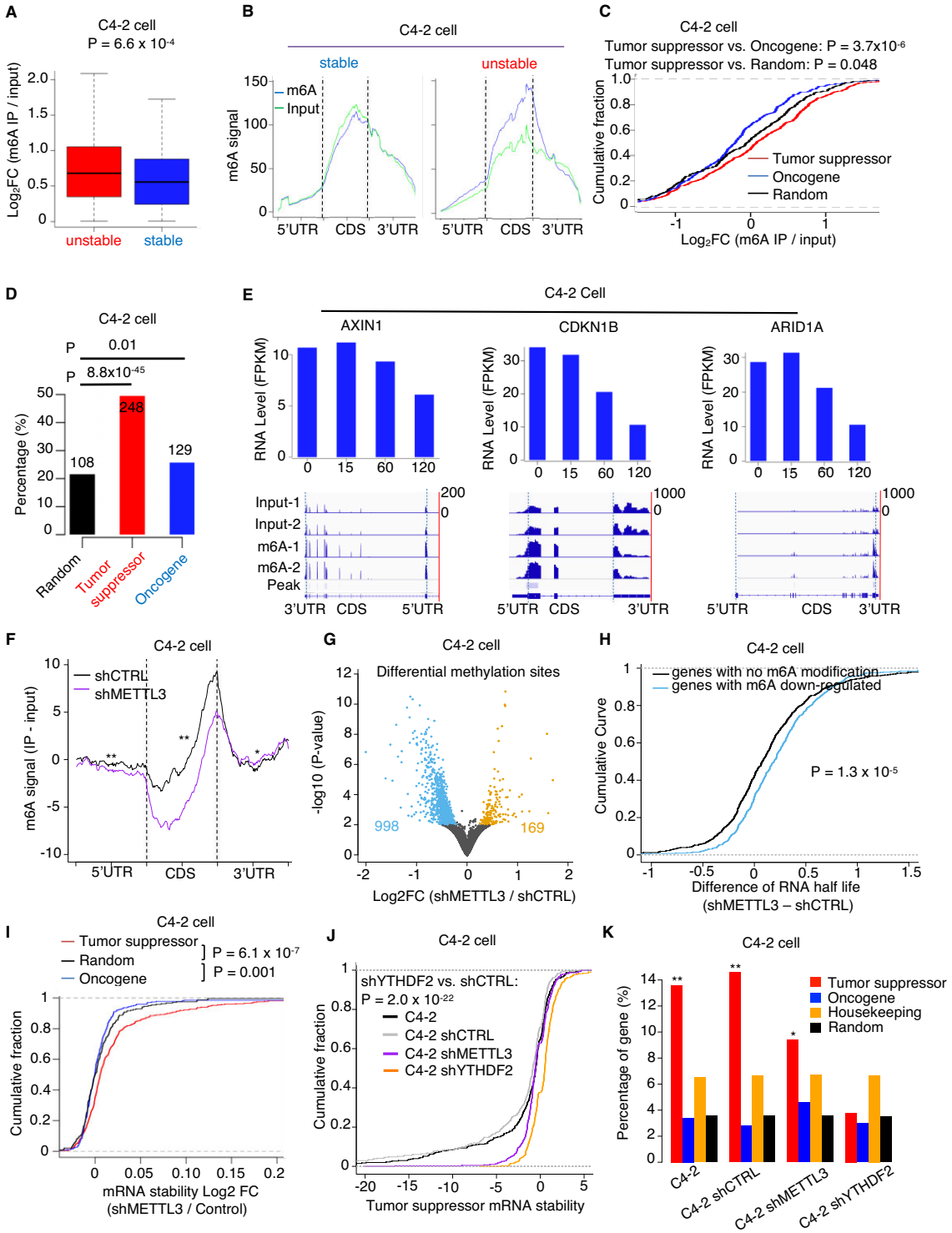

Figure 3. Low RNA stability of tumor suppressors is associated with preferential m^{6}A modification on their transcripts. (**A**) Boxplot to show fold enrichment of RNA m^{6}A modification on transcripts in C4-2 cells. (**B**) The m^{6}A signal distribution across the transcript divided into 5′ UTR, CDS and 3′ UTR regions. (**C**) Cumulative fraction of genes plotted against fold enrichment of m^{6}A modification on their transcripts. (**D**) Percentage of tumor suppressors, oncogenes and randomly selected control genes that showed m^{6}A peaks on their transcripts. (**E**) RNA expression level of individual genes at individual time points during inhibition of transcription (top panels) and genome browser tracks to show m^{6}A modification signal and peaks on transcripts of these genes (bottom panels). (**F**) The distribution of m^{6}A signal across transcripts divided into the 5′ UTR, CDS and 3′ UTR regions. (**G**) Volcano plot to show differential methylation sites between METTL3 knockdown and control samples. Number of differentially methylated sites are indicated. (**H**) Cumulative fraction of genes plotted as a function of difference in RNA half-life between METT3 knockdown and control C4-2 cells. (**I**) Cumulative fraction of genes plotted as a function of difference in RNA stability between METTL3 knockdown and control C4-2 cells. (**J**) Cumulative fraction of genes plotted as a function of RNA stability in individual samples. (**K**) Percentage of tumor suppressors, oncogenes, house-keeping genes, and randomly selected control genes in top 1000 genes of the most unstable transcripts from individual samples. $^{**}P$ value $< 1 \times 10^{-10}$. $^{*}P$ value $< 1 \times 10^{-3}$. *P* values were calculated by two tails Wilcoxon test (A, F), one tail K–S test (C, H, I, J), and one tail Fisher's exact test (D, K). When applicable, *P* values were adjusted by the Bonferroni method (K).

(Supplementary Figure S10C). The result showed that the protein expression of all these genes was increased upon METTL3 KD and YTHDF2 KD (Supplementary Figure S10A). These results suggested that tumor suppressors tended to have both higher RNA stability and higher protein abundance when METTL3 or YTHDF2 was knocked down.

METTL3 knockdown has no preferential impact on the nascent transcription of tumor suppressors

Recent studies have reported that nascent transcription can be regulated by METTL3 at the co-transcriptional level (31,57). To investigate the impact of METTL3 KD on nascent transcription of tumor suppressors, we analyzed a PRO-Seq dataset from MCF-7 cell line published by Xu *et al.* (31). The nascent transcription activity of tumor suppressors, oncogenes, and random control genes were calculated, and the result was shown in Supplementary Figure S11A. METTL3 KD caused a global reduction of nascent transcription, which is consistent with the result in the published paper (31). Interestingly, the degree of nascent transcription reduction upon METTL3 KD tended to be similar between tumor suppressors, oncogenes, and random control genes (Supplementary Figure S11A). This result indicated that the effects of METTL3 KD on nascent transcription regulation is not specific to any one of these three gene categories. However, METTL3 KD significantly increased RNA stability of tumor suppressors rather than that of oncogenes and random control genes (Supplementary Figure S11B). These results showed that the effect of METTL3 KD on RNA stability has a remarkable preference towards tumor suppressors, whereas the effect on nascent transcription did not show such preference.

We further conducted experiments to verify nascent transcription activity of tumor suppressors, oncogenes, and housekeeping genes in prostate cancer cells and normal prostate epithelial cells. In this experiment, nascent RNA was specifically isolated from total RNAs of prostate cancer cells (C4-2 cells) and normal epithelial cells (PrEC) with or without METTL3 KD (Supplementary Figure S11C–H). First, we tested four tumor suppressor genes, including *KLF4*, *BAX*, *CDKN1B* and *SETD7*. In response to the METTL3 KD in PrEC cells, nascent mRNA levels were modestly decreased for *KLF4* and *CDKN1B* but remain unchanged for *BAX* and *SETD7* (Supplementary Figure S11C). The nascent RNA levels of all four genes were not significantly changed in C4-2 cells upon METTL3 KD (Supplementary Figure S11D). Second, we tested the nascent transcription level of two oncogenes (*CARM1* and *PTPRA*). The result showed that the nascent RNA levels of both genes were decreased upon METTL3 KD in both PrEC (Supplementary Figure S11E) and C4-2 cells (Supplementary Figure S11F). Lastly, we further examined two housekeeping genes, *SUCLG1* and *ME2*. The result showed that nascent transcription levels of these housekeeping genes were not significantly changed in both PrEC cells (Supplementary Figure S11G) and C4-2 cells (Supplementary Figure S11H) upon METTL3 KD. Therefore, the effect observed in these experiments is less obvious when compared to that observed in the PRO-Seq data, which is likely because the PRO-Seq dataset of MCF-7 cells were generated with spike-ins as an external control. However, consistent with the observation in the PRO-seq data, our results confirmed that the effect of METTL3 KD on nascent transcription has no preference towards tumor suppressor genes when compared to oncogenes and random control genes.

m^{6}A-mediated decay of tumor suppressor RNAs is enhanced in cancer cells

Tumor suppressor expression level would be more likely to be downregulated in cancer cells relative to normal cells. We hypothesized that the expression downregulation could be mediated by increased m^{6}A modification. We thus performed a comparison between prostate normal epithelial cell PrEC and cancer cell C4-2. Our experiments showed that four m^{6}A writers (METTL3, METTL14, WTAP and VIRMA), three m^{6}A readers (YTHDF1, YTHDF2 and YTHDC1) and a m^{6}A eraser (ALKBH5) showed higher protein expression in C4-2 cells compared to PrEC, whereas only a m^{6}A eraser FTO showed lower protein abundance in C4-2 cells compared to PrEC (Supplementary Figure S12A). Further, global m^{6}A level in the cells was higher in C4-2 compared to PrEC (Supplementary Figure S12B). These results demonstrated that when compared to the normal cell PrEC, the prostate cancer cell C4-2 tended to have higher protein abundance of m^{6}A regulators and increased global m^{6}A levels.

Consistent with the observation in C4-2 cells (Figure 3B), m^{6}A modification in PrEC appeared more enriched on unstable RNAs than on stable RNAs (Figure 4A). Compared to the stable RNAs defined in PrEC, the unstable RNAs defined in PrEC cells showed a greater (one-tail Kolmogorov–Smirnov test $P = 0.0005$) increase of m^{6}A modification in C4-2 cells relative to PrEC (Figure 4B). Also, decrease of steady state RNA level in C4-2 cells relative to PrEC is greater (one-tail Kolmogorov-Smirnov test $P = 1.3 \times 10^{-35}$) for unstable RNAs than for stable RNAs defined in PrEC (Figure 4C). Therefore, unstable transcripts in the normal cell PrEC are preferentially down regulated in the cancer cell C4-2 through increase of m^{6}A modification.

Consistent with their low RNA stability, tumor suppressor RNAs are enriched with m^{6}A peaks in both PrEC (2.3-fold, one-tail Fisher's exact test $P = 5.3 \times 10^{-66}$) and C4-2 cells (2.0-fold, one-tail Fisher's exact test $P = 9.0 \times 10^{-53}$) (Figure 4D–F). For comparison, enrichment of m^{6}A peaks is significantly less on oncogenes than on tumor suppressors (Figure 4D–F). Intriguingly, this difference in m^{6}A modification between oncogenes and tumor suppressors were substantially amplified from PrEC to C4-2 cells (Figure 4G versus Figure 4H). Further, with the knockdown of METTL3 in C4-2 cells, the m^{6}A signal on RNAs of tumor suppressors were markedly reduced (Figure 4H versus Figure 4I). In contrast, the knockdown caused little change to m^{6}A on oncogenes.

In addition, m^{6}A peaks of tumor suppressor mRNAs were enriched in the CDS region near the stop codon (Figure 4G–I), which is consistent with previously reported enrichment pattern of m^{6}A peaks on the transcript body (14,15). Also, the enrichment of m^{6}A peaks near the stop codon was observed for unstable RNAs but not for stable RNAs (Supplementary Figure S13A and B). About 60% to 70% unstable RNAs contained m^{6}A peaks in CDS and 3′ UTR, while only 15–30% stable RNAs had m^{6}A peaks in these two regions (Supplementary Figure S13C). When comparing m^{6}A positional distribution between tumor suppressors and oncogenes, tumor suppressors showed higher m^{6}A levels in the whole transcript body, but with the greatest difference in CDS and 3′ UTR (Supplementary Figure S13D). The increase of m^{6}A on tumor

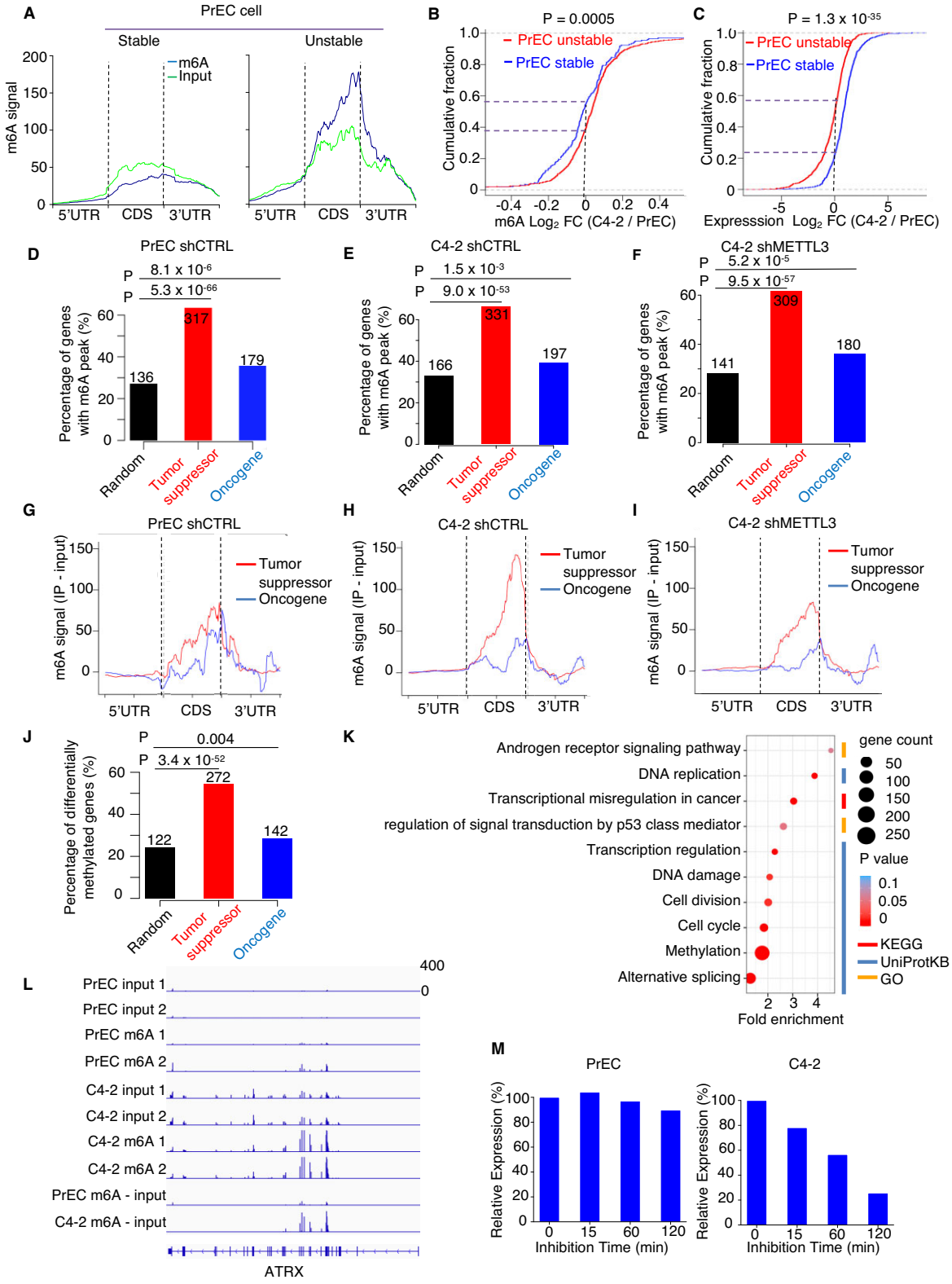

Figure 4. Decrease of tumor suppressor RNA stability in prostate cancer cells relative to normal cells. (**A**) Distribution of m^{6}A signal across transcripts in PrEC cells. (**B**)(**C**) Cumulative fraction of genes plotted against difference in m^{6}A signal (**B**) and expression level (**C**) between C4-2 and PrEC cells. (D–F) Percentage of tumor suppressors, oncogenes and randomly selected control genes that showed m^{6}A enrichment peaks in PrEC shCTRL cells (**D**), C4-2 shCTRL cells (**E**) and C4-2 shMETTL3 cells (**F**). (G–I) Distribution of m^{6}A signal across transcripts in PrEC shCTRL cells (**G**), C4-2 shCTRL cells (**H**) and C4-2 shMETTL3 cells (**I**). (**J**) Percentage of tumor suppressors, oncogenes and randomly selected control genes that showed differential m^{6}A modification sites between PrEC and C4-2 cells. (**K**) Functional enrichment analysis of genes that showed up-regulated of m^{6}A methylation in C4-2 shCTRL compared to PrEC shCTRL cells. (**L**) Genome browser tracks to show m^{6}A methylation signal on transcripts of ATRX, a tumor suppressor gene. (**M**) Relative RNA expression level of ATRX in C4-2 cells and PrEC cells at individual time points during inhibition of transcription. *P* values were calculated by one tail K–S test (B, C), and one tail Fisher's exact test (D–F, J).

suppressor mRNAs in C4-2 cells relative to PrEC was also most significant in the CDS region near the stop codon. Therefore, the CDS region near stop codon is the main target region of m^{6}A on tumor suppressors mRNAs.

The percentage of tumor suppressors showing differential m^{6}A methylation on their RNAs was significantly larger than that of randomly selected control genes (2.2-fold, one tailed Fisher's exact test $P = 3.4 \times 10^{-52}$) (Figure 4J). These results indicate that m^{6}A preferentially increase on tumor suppressor RNAs but not on oncogene RNAs in the cancer cell C4-2 when compared to PrEC. Functional enrichment analysis revealed that the genes showing upregulated m^{6}A methylation in C4-2 cells were enriched in cancer-related pathways (Figure 4K and Supplementary Table S7). These included pathways associated with androgen receptor signaling pathway, transcriptional misregulation in cancer, signal transduction by p53, and cell cycle. For instance, the tumor suppressor *ATRX* (58) showed a higher m^{6}A level in C4-2 cells when compared to PrEC (Figure 4L). Correspondingly, RNA degradation rate of *ATRX* was higher in C4-2 cells than in PrEC (Figure 4M).

Taken together, we conclude that the preferential m^{6}A modification on tumor suppressor RNAs contributed to a strong regulatability of tumor suppressor expression in cancer cells.

Factors other than m^{6}A might also contribute to the low RNA stability of tumor suppressors

It is worth noting that several other post-transcriptional regulatory mechanisms can potentially affect RNA stability of tumor suppressors. For instance, AU-rich elements and microRNAs are well-recognized regulators of RNA stability in various RNA molecules (59,60). Therefore, it is plausible that such additional factors may also mediate the instability of tumor suppressor RNAs. To test this hypothesis, we performed an analysis of AU-rich elements and microRNA binding sites in addition to m^{6}A. We first confirmed that both m^{6}A peaks and AU-rich elements were highly enriched in unstable RNAs compared to stable RNAs (Supplementary Figure S14A and C). Intriguingly, microRNAs binding sites were significantly enriched in both stable and unstable RNAs, although slightly more enriched in unstable RNAs (Supplementary Figure S14E). Thereafter, we examined the enrichment of these factors on tumor suppressors and found that all of them were significantly enriched (Supplementary Figure S14B, D, F). Therefore, it is likely that multiple RNA stability regulators, including but not limited to m^{6}A methylation, AU-rich elements, and microRNAs, may also contribute to the instability of tumor suppressor RNAs. Although our work is focused on the crucial role of m^{6}A methylation in regulating RNA stability of tumor suppressors, further investigations are warranted to explore the involvement of other RNA stability regulators in this phenomenon.

Discussion

In this study, we uncovered a unique RNA turnover signature for tumor suppressors. We observed both strong signals of transcription activity and fast RNA decay for tumor suppressors. This reflects faster RNA turnover rate of tumor suppressors compared to other genes such as housekeeping genes in the cells. In this process, m^{6}A plays an important role in mediating the low RNA stability of tumor suppressors. This interesting finding was recaptured in multiple different cell types, indicating that it is a mechanism conserved across cell types.

Our statistical analysis demonstrated that tumor suppressors are significantly more enriched with m^{6}A when compared to oncogenes and random control genes. However, this statistical significance does not exclude the possibility that a few oncogenes might be regulated by m^{6}A in some specific biological contexts. For instance, we did observe that oncogenes are slightly enriched (1.19-fold, $P = 0.01$) with m^{6}A sites in the C4-2 cells. However, the enrichment is much less significant when compared to that of tumor suppressors (2.30-fold, $P = 8.8 \times 10^{-45}$). Further, the modification frequency on m^{6}A sites appeared to be overall weaker for oncogenes when compared to tumor suppressors and random control genes. These results indicated that oncogenes do have m^{6}A sites, but the modification at these sites is significantly less frequent when compared to other genes, suggesting that the mechanism regulating the modification at these m^{6}A sites might be different. As an example, *MYC* is an oncogene with a wide range of functions involving cell cycle, apoptosis, DNA damage, hematopoiesis, and so on (61). We observed that the *MYC* mRNA has m^{6}A peaks in both the normal cells PrEC and the cancer cells C4-2 in our MeRIP-Seq data (Supplementary Figure S15). Intriguingly, Huang et. al. reported that *MYC* is enriched with m^{6}A modification and can be recognized by the m^{6}A reader IGF2BP, which could enhance its RNA stability (23). Zhao et. al. also found that m^{6}A modification in *MYC* enhanced the mRNA stability mediated by YTHDF1 in OSCC (62). Meanwhile, a previous study demonstrated that the instability of *MYC* can be caused by AU-rich element (63). Therefore, it is likely that the relationship between m^{6}A modification and RNA instability of *MYC* are mediated by different mechanisms in these contexts. Despite of such individual examples of m^{6}A on mRNAs of oncogenes in specific contexts, the statistical enrichment of m^{6}A on mRNAs of oncogenes is slight and far less significant when compared to that of tumor suppressors. Taken together, our data support the conclusion that tumor suppressors tend to be significantly more enriched with m^{6}A methylation compared to oncogenes and random control genes.

There might be a yet unclear mechanism underlying the specificity and selectivity of METTL3 activity on RNAs of tumor suppressors. We observed that RNAs of tumor suppressors are more prone to m^{6}A modification when compared with RNAs of other genes such as oncogenes and housekeeping genes. Further, the RNAs of tumor suppressors are more vulnerable to the alteration of the m^{6}A methyltransferase METTL3. It will be interesting to define RNA sequence elements that might recruit m^{6}A writers to the RNAs of tumor suppressors. Such regulatory elements might recruit m^{6}A writers directly or indirectly through other potential RNA-binding proteins. Such a mechanism of preferential m^{6}A modification on RNAs of tumor suppressors is yet largely unclear. However, previous studies have proposed models that might guide specificity of m^{6}A modification. For instance, m^{6}A specificity may be mediated by histone modifications on chromatin, the binding of transcription factors on enhancer DNA, or some RNA-binding proteins interacting with the METTL3-METTL14 complex (64). Histone modification patterns on tumor suppressor genes in a normal cell tend to be different from those on other genes such as housekeeping genes. For instance, H3K4me3 tend to have a broad enrichment pattern on tumor suppressor genes but a sharp enrichment pattern on housekeeping genes (65). Whereas sharp H3K4me3 is

associated with transcription initiation, the broad H3K4me3 is associated with transcription elongation (65). Another histone modification, H3K36me3, is a well-known marker of transcription elongation. Notably, H3K36me3 was reported to guide the recruitment of the m^{6}A writer complex to specific DNA locations and thus facilitate co-transcriptional m^{6}A modification on RNAs (66). Meanwhile, it is reported that METTL3 could bind to chromatin in regions carrying H3K4me3 modification (67). Intriguingly, a recent study in our lab reported significant enrichment of super enhancers and broad H3K4me3 modifications at the gene loci of unstable RNAs. Meanwhile, METTL3 can preferentially bind to super enhancers and broad H3K4me3 on these loci, and this binding pattern positively correlated with m^{6}A methylation and negatively correlated with RNA stability of the methylated genes. Therefore, it is possible that the broad H3K4me3 of tumor suppressor genes might guide a preferential binding of METTL3 on tumor suppressor genes. This mechanism may potentially facilitate preferential co-transcriptional m^{6}A modification on tumor suppressor RNAs. This hypothesis would require comprehensive molecular and biochemical experiments to validate in future. Intriguingly, genes involved in the regulation of alternative splicing were enriched in the genes of mRNAs differentially methylated between cancer and normal (Figure 4K). These include 263 genes, such as the *LUC7L3*, *SON*, *SCAF11*, *THOC2*, etc. It will be interesting to understand in future how the regulation of these genes by m^{6}A put an effect on RNA alternative splicing, which is frequently reported in cancer (68).

Transcription and RNA decay are two important processes controlling the RNA level of gene expression at the transcriptional and post-transcriptional levels, respectively. Investigation of gene expression regulation at the transcriptional level has revealed multiple unique epigenetic modification signatures on chromatin, e.g. super enhancers (69–71), broad H3K4me3 (65), DNA methylation canyons (72), BLOCKs (73), LOCKs (74), broad genic repression domains (BGRD), and broad H3K27me3 (6). Some of these signatures were each found to preferentially regulate a unique functional category of genes. For instance, whereas super enhancers and cell type specific broad H3K4me3 were found to regulate cell identity genes, the broad H3K4me3 conserved between cell types were found to regulate tumor suppressor genes (5,69,70). Further, the BGRD conserved between cell types were found to regulate oncogenes (6). However, little is yet known about the unique pattern of post-transcriptional regulation for a functional category of genes. To the best of our knowledge, this work revealed for the first time an m^{6}A-mediated unique RNA decay pattern in post-transcriptional regulation of tumor suppressor genes.

The findings from this study could have a promising implication in the discovery of potential therapeutic targets for cancer treatment. The rapid turnover, low RNA stability, and preferential m^{6}A modification of tumor suppressor RNAs might be useful features to uncover new tumor suppressor genes. The false positive rate might be high if simply using each of these features without a further manual curation. However, accuracy might be significantly improved in future by combining a set of such features in an optimal manner using a machine learning model. The m^{6}A levels of tumor suppressors are markedly higher in the prostate cancer cells compared to normal prostate epithelial cells. The m^{6}A writer protein METTL3 is up regulated in prostate cancers. Knockdown of the m^{6}A 'writer' METTL3 and 'reader' YTHDF2 in cancer cells preferentially improve stability of tumor suppressor RNAs. Therefore, tumor suppressor RNAs could be more vulnerable to the manipulation of RNA stability regulators. It might be promising to target these regulators to develop new therapy in future.

The new insights obtained from this work highlighted the importance of RNA turnover rate analysis. Steady-state RNA expression level couldn't reflect the dynamic turnover of transcripts. Genes with a similar steady-state RNA expression level can have dramatically different transcription rate and RNA decay rate. Maintaining a fast turnover of some transcripts might be pivotal for the ability of cells to rapidly respond to environment signals and stresses. The individual patterns of RNA turnover, including both transcription and degradation, could denote unique biological implications. Genes with the same RNA turnover pattern might represent a group of genes sharing common function and expression regulation mechanism. For example, the observed frequent transcription and fast decay of tumor suppressor genes in this study. An analysis of steady state RNA level alone will not be able to reveal such biological implication. Therefore, the discovery in this work indicated the significance for the community to investigate RNA turnover in numerous biological and disease models.

Data availability

The datasets supporting the conclusions of this article are included within the article and its supplementary material. The RNA-seq and MeRIP-seq newly generated in this study were deposited into the GEO database with the accession number GSE197495. GEO accession numbers of public datasets used in this manuscript were listed in Supplementary Table S3. The computational codes and the processed data that were used to generate individual figures were deposited to https://doi.org/10.6084/m9.figshare.19346171.v2.

Supplementary data

Supplementary Data are available at NAR Online.

Acknowledgements

We would like to thank all researchers who generated the public genomic datasets analyzed in this study.

Author contributions: K.C. conceived the project. X.G., J.L. and K.C. designed the analysis and interpreted the data. Y.Y. designed and performed the experiments under the supervision of Q.C.. X.G. and J.L. performed the data analysis. Y.Y. conducted RNA-seq and MeRIP-seq experiments for PrEC and C4-2 cells. S.B. and I.B. performed T cell RNA-Seq. K.C., X.G. and J.L. wrote the manuscript with comments from Q.C., Y.Y., Y.L., K.A. and L.Z.

Funding

NIH [R01GM138407, R01GM125632, R01HL148338 to K.C., R01HL155632 to L.Z., R01CA256741, R01CA208257 to Q.C., in part]; L.Z. is further supported by a Single Ventricle Research Foundation grant from the Additional Ventures; Q.C. is further supported by U.S. Department of Defense [W81XWH-17–1-0357, W81XWH-19–1-0563, W81XWH-20–1-0504]; American Cancer Society [RSG-15–192-01]; Prostate SPORE [P50CA180995 Developmental Research Program]; Polsky Urologic Cancer Institute of the

Robert H. Lurie Comprehensive Cancer Center of Northwestern University at Northwestern Memorial Hospital. Funding for open access charge: NIH [R01GM138407, GM125632, R01HL148338 to K.C.].

Conflict of interest statement

None declared.

References

1. Hanahan,D. and Weinberg,R.A. (2000) The hallmarks of cancer. *Cell*, **100**, 57–70.
2. Hanahan,D. and Weinberg,R.A. (2011) Hallmarks of cancer: the next generation. *Cell*, **144**, 646–674.
3. Vogelstein,B., Papadopoulos,N., Velculescu,V.E., Zhou,S., Diaz,L.A. Jr and Kinzler,K.W. (2013) Cancer genome landscapes. *Science*, **339**, 1546–1558.
4. Li,E. (2002) Chromatin modification and epigenetic reprogramming in mammalian development. *Nat. Rev. Genet.*, **3**, 662–673.
5. Chen,K., Chen,Z., Wu,D., Zhang,L., Lin,X., Su,J., Rodriguez,B., Xi,Y., Xia,Z., Chen,X., *et al.* (2015) Broad H3K4me3 is associated with increased transcription elongation and enhancer activity at tumor-suppressor genes. *Nat. Genet.*, **47**, 1149–1157.
6. Zhao,D., Zhang,L., Zhang,M., Xia,B., Lv,J., Gao,X., Wang,G., Meng,Q., Yi,Y., Zhu,S., *et al.* (2020) Broad genic repression domains signify enhanced silencing of oncogenes. *Nat. Commun.*, **11**, 5560.
7. Su,J., Huang,Y.H., Cui,X., Wang,X., Zhang,X., Lei,Y., Xu,J., Lin,X., Chen,K., Lv,J., *et al.* (2018) Homeobox oncogene activation by pan-cancer DNA hypermethylation. *Genome Biol.*, **19**, 108.
8. Mitchell,P. and Tollervey,D. (2001) mRNA turnover. *Curr. Opin. Cell Biol.*, **13**, 320–325.
9. Vilborg,A., Glahder,J.A., Wilhelm,M.T., Bersani,C., Corcoran,M., Mahmoudi,S., Rosenstierne,M., Grander,D., Farnebo,M., Norrild,B., *et al.* (2009) The p53 target Wig-1 regulates p53 mRNA stability through an AU-rich element. *Proc. Natl. Acad. Sci. U.S.A.*, **106**, 15756–15761.
10. Hollams,E.M., Giles,K.M., Thomson,A.M. and Leedman,P.J. (2002) MRNA stability and the control of gene expression: implications for human disease. *Neurochem. Res.*, **27**, 957–980.
11. Steinman,R.A. (2007) mRNA stability control: a clandestine force in normal and malignant hematopoiesis. *Leukemia*, **21**, 1158–1171.
12. Perron,G., Jandaghi,P., Solanki,S., Safisamghabadi,M., Storoz,C., Karimzadeh,M., Papadakis,A.I., Arseneault,M., Scelo,G., Banks,R.E., *et al.* (2018) A general framework for interrogation of mRNA stability programs identifies RNA-binding proteins that govern cancer transcriptomes. *Cell Rep.*, **23**, 1639–1650.
13. Wei,C.M., Gershowitz,A. and Moss,B. (1975) Methylated nucleotides block 5′ terminus of HeLa cell messenger RNA. *Cell*, **4**, 379–386.
14. Dominissini,D., Moshitch-Moshkovitz,S., Schwartz,S., Salmon-Divon,M., Ungar,L., Osenberg,S., Cesarkas,K., Jacob-Hirsch,J., Amariglio,N., Kupiec,M., *et al.* (2012) Topology of the human and mouse m^6A RNA methylomes revealed by m^6A-seq. *Nature*, **485**, 201–206.
15. Meyer,K.D., Saletore,Y., Zumbo,P., Elemento,O., Mason,C.E. and Jaffrey,S.R. (2012) Comprehensive analysis of mRNA methylation reveals enrichment in 3′ UTRs and near stop codons. *Cell*, **149**, 1635–1646.
16. Wang,X., Lu,Z., Gomez,A., Hon,G.C., Yue,Y., Han,D., Fu,Y., Parisien,M., Dai,Q., Jia,G., *et al.* (2014) N6-methyladenosine-dependent regulation of messenger RNA stability. *Nature*, **505**, 117–120.
17. Kim,D., Pertea,G., Trapnell,C., Pimentel,H., Kelley,R. and Salzberg,S.L. (2013) TopHat2: accurate alignment of transcriptomes in the presence of insertions, deletions and gene fusions. *Genome Biol.*, **14**, R36.
18. Trapnell,C., Hendrickson,D.G., Sauvageau,M., Goff,L., Rinn,J.L. and Pachter,L. (2013) Differential analysis of gene regulation at transcript resolution with RNA-seq. *Nat. Biotechnol.*, **31**, 46–53.
19. Robinson,M.D., McCarthy,D.J. and Smyth,G.K. (2010) edgeR: a Bioconductor package for differential expression analysis of digital gene expression data. *Bioinformatics*, **26**, 139–140.
20. Robinson,J.T., Thorvaldsdottir,H., Winckler,W., Guttman,M., Lander,E.S., Getz,G. and Mesirov,J.P. (2011) Integrative genomics viewer. *Nat. Biotechnol.*, **29**, 24–26.
21. Fisher,R.A. (1932) In: *Statistical Methods for Research Workers*. 5th edn., Oliver and Boyd, Edinburgh.
22. Neri,F., Rapelli,S., Krepelova,A., Incarnato,D., Parlato,C., Basile,G., Maldotti,M., Anselmi,F. and Oliviero,S. (2017) Intragenic DNA methylation prevents spurious transcription initiation. *Nature*, **543**, 72–77.
23. Huang,H., Weng,H., Sun,W., Qin,X., Shi,H., Wu,H., Zhao,B.S., Mesquita,A., Liu,C., Yuan,C.L., *et al.* (2018) Recognition of RNA N(6)-methyladenosine by IGF2BP proteins enhances mRNA stability and translation. *Nat. Cell Biol.*, **20**, 285–295.
24. Dennis,G. Jr, Sherman,B.T., Hosack,D.A., Yang,J., Gao,W., Lane,H.C. and Lempicki,R.A. (2003) DAVID: database for annotation, visualization, and integrated discovery. *Genome Biol.*, **4**, P3.
25. Bolger,A.M., Lohse,M. and Usadel,B. (2014) Trimmomatic: a flexible trimmer for Illumina sequence data. *Bioinformatics*, **30**, 2114–2120.
26. Langmead,B., Trapnell,C., Pop,M. and Salzberg,S.L. (2009) Ultrafast and memory-efficient alignment of short DNA sequences to the human genome. *Genome Biol.*, **10**, R25.
27. Zhang,Y., Liu,T., Meyer,C.A., Eeckhoute,J., Johnson,D.S., Bernstein,B.E., Nusbaum,C., Myers,R.M., Brown,M., Li,W., *et al.* (2008) Model-based analysis of ChIP-Seq (MACS). *Genome Biol.*, **9**, R137.
28. Chen,K., Xi,Y., Pan,X., Li,Z., Kaestner,K., Tyler,J., Dent,S., He,X. and Li,W. (2013) DANPOS: dynamic analysis of nucleosome position and occupancy by sequencing. *Genome Res.*, **23**, 341–351.
29. Xia,B., Zhao,D., Wang,G., Zhang,M., Lv,J., Tomoiaga,A.S., Li,Y., Wang,X., Meng,S., Cooke,J.P., *et al.* (2020) Machine learning uncovers cell identity regulator by histone code. *Nat. Commun.*, **11**, 2696.
30. Ramirez,F., Ryan,D.P., Gruning,B., Bhardwaj,V., Kilpert,F., Richter,A.S., Heyne,S., Dundar,F. and Manke,T. (2016) deepTools2: a next generation web server for deep-sequencing data analysis. *Nucleic Acids Res.*, **44**, W160–W165.
31. Xu,W., He,C., Kaye,E.G., Li,J., Mu,M., Nelson,G.M., Dong,L., Wang,J., Wu,F., Shi,Y.G., *et al.* (2022) Dynamic control of chromatin-associated m(6)A methylation regulates nascent RNA synthesis. *Mol. Cell*, **82**, 1156–1168.
32. Chen,S., Zhou,Y., Chen,Y. and Gu,J. (2018) fastp: an ultra-fast all-in-one FASTQ preprocessor. *Bioinformatics*, **34**, i884–i890.
33. 1000 Genome Project Data Processing Subgroup, Li,H., Handsaker,B., Wysoker,A., Fennell,T., Ruan,J., Homer,N., Marth,G., Abecasis,G. and Durbin,R.(2009) The Sequence Alignment/Map format and SAMtools. *Bioinformatics*, **25**, 2078–2079.
34. Anders,S., Pyl,P.T. and Huber,W. (2015) HTSeq–a Python framework to work with high-throughput sequencing data. *Bioinformatics*, **31**, 166–169.
35. Chang,B.L., Zheng,S.L., Isaacs,S.D., Wiley,K.E., Turner,A., Li,G., Walsh,P.C., Meyers,D.A., Isaacs,W.B. and Xu,J. (2004) A polymorphism in the CDKN1B gene is associated with increased risk of hereditary prostate cancer. *Cancer Res.*, **64**, 1997–1999.
36. Feng,X., Lu,T., Li,J., Yang,R., Hu,L., Ye,Y., Mao,F., He,L., Xu,J., Wang,Z., *et al.* (2020) The tumor suppressor interferon regulatory factor 2 binding protein 2 regulates hippo pathway in liver cancer by a feedback loop in mice. *Hepatology*, **71**, 1988–2004.
37. Eisenberg,E. and Levanon,E.Y. (2013) Human housekeeping genes, revisited. *Trends Genet.*, **29**, 569–574.

38. Rohn,G., Koch,A., Krischek,B., Stavrinou,P., Goldbrunner,R. and Timmer,M. (2018) ACTB and SDHA are suitable endogenous reference genes for gene expression studies in human astrocytomas using quantitative RT-PCR. *Technol. Cancer Res. Treat.*, **17**, 1533033818802318.
39. Davoli,T., Xu,A.W., Mengwasser,K.E., Sack,L.M., Yoon,J.C., Park,P.J. and Elledge,S.J. (2013) Cumulative haploinsufficiency and triplosensitivity drive aneuploidy patterns and shape the cancer genome. *Cell*, **155**, 948–962.
40. Malumbres,M. and Barbacid,M. (2009) Cell cycle, CDKs and cancer: a changing paradigm. *Nat. Rev. Cancer*, **9**, 153–166.
41. Siu,M.K., Suau,F., Chen,W.Y., Tsai,Y.C., Tsai,H.Y., Yeh,H.L. and Liu,Y.N. (2016) KLF4 functions as an activator of the androgen receptor through reciprocal feedback. *Oncogenesis*, **5**, e282.
42. Yang,W.T. and Zheng,P.S. (2014) Promoter hypermethylation of KLF4 inactivates its tumor suppressor function in cervical carcinogenesis. *PLoS One*, **9**, e88827.
43. Jia,X., Li,L., Wang,F., Xue,Y., Wu,T., Jia,Q., Li,Y., Wu,C., Chen,Y., Wu,J., *et al.* (2022) DUB3/KLF4 combats tumor growth and chemoresistance in hepatocellular carcinoma. *Cell Death Discov.*, **8**, 166.
44. Rowland,B.D., Bernards,R. and Peeper,D.S. (2005) The KLF4 tumour suppressor is a transcriptional repressor of p53 that acts as a context-dependent oncogene. *Nat. Cell Biol.*, **7**, 1074–1082.
45. Yori,J.L., Seachrist,D.D., Johnson,E., Lozada,K.L., Abdul-Karim,F.W., Chodosh,L.A., Schiemann,W.P. and Keri,R.A. (2011) Kruppel-like factor 4 inhibits tumorigenic progression and metastasis in a mouse model of breast cancer. *Neoplasia*, **13**, 601–610.
46. Goler-Baron,V., Selitrennik,M., Barkai,O., Haimovich,G., Lotan,R. and Choder,M. (2008) Transcription in the nucleus and mRNA decay in the cytoplasm are coupled processes. *Genes Dev.*, **22**, 2022–2027.
47. Dong,X. and Weng,Z. (2013) The correlation between histone modifications and gene expression. *Epigenomics*, **5**, 113–116.
48. Komarnitsky,P., Cho,E.J. and Buratowski,S. (2000) Different phosphorylated forms of RNA polymerase II and associated mRNA processing factors during transcription. *Genes Dev.*, **14**, 2452–2460.
49. Wu,X. and Brewer,G. (2012) The regulation of mRNA stability in mammalian cells: 2.0. *Gene*, **500**, 10–21.
50. Roundtree,I.A., Evans,M.E., Pan,T. and He,C. (2017) Dynamic RNA modifications in gene expression regulation. *Cell*, **169**, 1187–1200.
51. Barbieri,I. and Kouzarides,T. (2020) Role of RNA modifications in cancer. *Nat. Rev. Cancer*, **20**, 303–322.
52. Satoh,S., Daigo,Y., Furukawa,Y., Kato,T., Miwa,N., Nishiwaki,T., Kawasoe,T., Ishiguro,H., Fujita,M., Tokino,T., *et al.* (2000) AXIN1 mutations in hepatocellular carcinomas, and growth suppression in cancer cells by virus-mediated transfer of AXIN1. *Nat. Genet.*, **24**, 245–250.
53. Wiegand,K.C., Shah,S.P., Al-Agha,O.M., Zhao,Y., Tse,K., Zeng,T., Senz,J., McConechy,M.K., Anglesio,M.S., Kalloger,S.E., *et al.* (2010) ARID1A mutations in endometriosis-associated ovarian carcinomas. *N. Engl. J. Med.*, **363**, 1532–1543.
54. Liu,J., Yue,Y., Han,D., Wang,X., Fu,Y., Zhang,L., Jia,G., Yu,M., Lu,Z., Deng,X., *et al.* (2014) A METTL3-METTL14 complex mediates mammalian nuclear RNA N6-adenosine methylation. *Nat. Chem. Biol.*, **10**, 93–95.
55. Shi,H., Wang,X., Lu,Z., Zhao,B.S., Ma,H., Hsu,P.J., Liu,C. and He,C. (2017) YTHDF3 facilitates translation and decay of N(6)-methyladenosine-modified RNA. *Cell Res.*, **27**, 315–328.
56. Yi,Y., Li,Y., Meng,Q., Li,Q., Li,F., Lu,B., Shen,J., Fazli,L., Zhao,D., Li,C., *et al.* (2021) A PRC2-independent function for EZH2 in regulating rRNA 2′-O methylation and IRES-dependent translation. *Nat. Cell Biol.*, **23**, 341–354.
57. Liu,J., Dou,X., Chen,C., Chen,C., Liu,C., Xu,M.M., Zhao,S., Shen,B., Gao,Y., Han,D., *et al.* (2020) N (6)-methyladenosine of chromosome-associated regulatory RNA regulates chromatin state and transcription. *Science*, **367**, 580–586.
58. Koschmann,C., Calinescu,A.A., Nunez,F.J., Mackay,A., Fazal-Salom,J., Thomas,D., Mendez,F., Kamran,N., Dzaman,M., Mulpuri,L., *et al.* (2016) ATRX loss promotes tumor growth and impairs nonhomologous end joining DNA repair in glioma. *Sci. Transl. Med.*, **8**, 328ra328.
59. Barreau,C., Paillard,L. and Osborne,H.B. (2005) AU-rich elements and associated factors: are there unifying principles?*Nucleic Acids Res.*, **33**, 7138–7150.
60. Valencia-Sanchez,M.A., Liu,J., Hannon,G.J. and Parker,R. (2006) Control of translation and mRNA degradation by miRNAs and siRNAs. *Genes Dev.*, **20**, 515–524.
61. Ahmadi,S.E., Rahimi,S., Zarandi,B., Chegeni,R. and Safa,M. (2021) MYC: a multipurpose oncogene with prognostic and therapeutic implications in blood malignancies. *J. Hematol. Oncol.*, **14**, 121.
62. Zhao,W., Cui,Y., Liu,L., Ma,X., Qi,X., Wang,Y., Liu,Z., Ma,S., Liu,J. and Wu,J. (2020) METTL3 facilitates oral squamous cell carcinoma tumorigenesis by enhancing c-Myc stability via YTHDF1-mediated m(6)A modification. *Mol. Ther. Nucleic Acids*, **20**, 1–12.
63. Brewer,G. (1991) An A + U-rich element RNA-binding factor regulates c-myc mRNA stability in vitro. *Mol. Cell. Biol.*, **11**, 2460–2466.
64. Zaccara,S., Ries,R.J. and Jaffrey,S.R. (2019) Reading, writing and erasing mRNA methylation. *Nat. Rev. Mol. Cell Biol.*, **20**, 608–624.
65. Chen,K.F., Chen,Z., Wu,D.Y., Zhang,L.L., Lin,X.Q., Su,J.Z., Rodriguez,B., Xi,Y.X., Xia,Z., Chen,X., *et al.* (2015) Broad H3K4me3 is associated with increased transcription elongation and enhancer activity at tumor-suppressor genes. *Nat. Genet.*, **47**, 1149–1157.
66. Huang,H., Weng,H., Zhou,K., Wu,T., Zhao,B.S., Sun,M., Chen,Z., Deng,X., Xiao,G., Auer,F., *et al.* (2019) Histone H3 trimethylation at lysine 36 guides m(6)A RNA modification co-transcriptionally. *Nature*, **567**, 414–419.
67. Huang,H., Weng,H., Zhou,K., Wu,T., Zhao,B.S., Sun,M., Chen,Z., Deng,X., Xiao,G. and Auer,F. (2019) Histone H3 trimethylation at lysine 36 guides m 6 A RNA modification co-transcriptionally. *Nature*, **567**, 414–419.
68. Bonnal,S.C., Lopez-Oreja,I. and Valcarcel,J. (2020) Roles and mechanisms of alternative splicing in cancer - implications for care. *Nat. Rev. Clin. Oncol.*, **17**, 457–474.
69. Whyte,W.A., Orlando,D.A., Hnisz,D., Abraham,B.J., Lin,C.Y., Kagey,M.H., Rahl,P.B., Lee,T.I. and Young,R.A. (2013) Master transcription factors and mediator establish super-enhancers at key cell identity genes. *Cell*, **153**, 307–319.
70. Hnisz,D., Abraham,B.J., Lee,T.I., Lau,A., Saint-Andre,V., Sigova,A.A., Hoke,H.A. and Young,R.A. (2013) Super-enhancers in the control of cell identity and disease. *Cell*, **155**, 934–947.
71. Loven,J., Hoke,H.A., Lin,C.Y., Lau,A., Orlando,D.A., Vakoc,C.R., Bradner,J.E., Lee,T.I. and Young,R.A. (2013) Selective inhibition of tumor oncogenes by disruption of super-enhancers. *Cell*, **153**, 320–334.
72. Jeong,M., Sun,D., Luo,M., Huang,Y., Challen,G.A., Rodriguez,B., Zhang,X., Chavez,L., Wang,H., Hannah,R., *et al.* (2014) Large conserved domains of low DNA methylation maintained by Dnmt3a. *Nat. Genet.*, **46**, 17–23.
73. Timp,W., Bravo,H.C., McDonald,O.G., Goggins,M., Umbricht,C., Zeiger,M., Feinberg,A.P. and Irizarry,R.A. (2014) Large hypomethylated blocks as a universal defining epigenetic alteration in human solid tumors. *Genome Med.*, **6**, 61.
74. Wen,B., Wu,H., Shinkai,Y., Irizarry,R.A. and Feinberg,A.P. (2009) Large histone H3 lysine 9 dimethylated chromatin blocks distinguish differentiated from embryonic stem cells. *Nat. Genet.*, **41**, 246–250.

Received: April 25, 2023. **Revised:** September 12, 2023. **Editorial Decision:** September 15, 2023. **Accepted:** September 20, 2023